



# Cadomian (Ediacaran–Cambrian) arc magmatism in the ChahJam–Biarjmand metamorphic complex (Iran): Magmatism along the northern active margin of Gondwana



Hadi Shafaii Moghadam <sup>a,\*</sup>, Mohsen Khademi <sup>a</sup>, Zhaochu Hu <sup>b</sup>, Robert J. Stern <sup>c</sup>, Jose F. Santos <sup>d</sup>, Yuanbao Wu <sup>e</sup>

<sup>a</sup> School of Earth Sciences, Damghan University, Damghan 36716–41167, Iran

<sup>b</sup> State Key Laboratory of Geological Processes and Mineral Resources, China University of Geosciences, Wuhan 430074, PR China

<sup>c</sup> Geosciences Dept., University of Texas at Dallas, Richardson, TX 75083–0688, USA

<sup>d</sup> Geobiotec, Departamento de Geociências, Universidade de Aveiro, 3810–193 Aveiro, Portugal

<sup>e</sup> Faculty of Earth Sciences, China University of Geosciences, Wuhan 430074, PR China

## ARTICLE INFO

### Article history:

Received 15 August 2013

Received in revised form 19 October 2013

Accepted 21 October 2013

Available online 27 November 2013

Handling Editor: R.D. Nance

### Keywords:

Cadomian magmatism

U–Pb dating

Zircon Hf isotopes

Gondwana

Iran

## ABSTRACT

The ChahJam–Biarjmand complex (CJBC), flanked by the Alborz Mountains in the north and the Lut–Tabas block to the south, is part of Central Iranian block, where the oldest continental crust of Iran is found. This complex contains granitic to tonalitic orthogneissic rocks (old plutons) and associated metasediments, amphibolites and paragneisses. Metamorphosed granitic and granodioritic dikes intrude orthogneisses as well as metasediments and are abundant close to the plutons (orthogneissic rocks). Based on the results of bulk rock trace and rare earth elements, the orthogneissic rocks are inferred to have crystallized from subduction-related melts. Amphibolites also have subduction-related signatures and are inferred to have formed both as metamorphosed volcanoclastic sediments and as attenuated basic dikes. The presence of para-amphibolites associated with paragneisses and metasediments (mica schists) could represent a sedimentary basin filled with magmatic arc erosional products. U–Pb zircon dating of the ChahJam–Biarjmand rocks yielded <sup>238</sup>U/<sup>206</sup>Pb crystallization ages of ca. 550 to 530 Ma (Ediacaran–early Cambrian). Sr–Nd isotope systematics on whole rocks ( $\epsilon_{\text{Nd}}(t) = -2.2$  to  $-5.5$ ) and zircon Hf isotope results indicate that CJBC Cadomian granitic rocks contain older, possible Mesoproterozoic, continental crust in their source. The ChahJam–Biarjmand granitic–tonalitic gneissic rocks are coeval with other similar-aged metagranites and gneisses within Iranian basement exposed in Central Iran, the Sanandaj–Sirjan Zone and the Alborz Mountains, as well as in the Tauride–Anatolide platform in western Anatolia and in NW Turkey. All these dispersed Cadomian basement rocks are interpreted to show fragments of Neoproterozoic–early Cambrian continental arcs bordering the northern active margin of Gondwana.

© 2013 International Association for Gondwana Research. Published by Elsevier B.V. All rights reserved.

## 1. Introduction

The Alpine–Himalayan orogenic belt in Europe and Asia includes peri-Gondwana terranes generated by Ediacaran–Cambrian arc-type magmatism typical of the Cadomian event (e.g., Fernández-Suárez et al., 2000, 2002; Nance et al., 2002; Ustaömer et al., 2009; Ustaömer et al., 2011). Ediacaran–Cambrian magmatism of the Cadomian belt is suggested to reflect widespread continental arc magmatism along the northern margin of Gondwana (e.g., Ramezani and Tucker, 2003; Ustaömer et al., 2009, 2011). Fragments of the Cadomian belt rifted from Gondwana during Cambrian–Ordovician times and accreted to Eurasia throughout the later Phanerozoic (e.g., Stampfli et al., 2002; Murphy et al., 2004; Nance et al., 2008, 2010; Ustaömer et al., 2011). Recent efforts to understand the Cadomian basement in Turkey and Iran emphasize dating of metamorphosed granites and gneissic rocks

and provenance analysis of Paleozoic sedimentary units (e.g., Ramezani and Tucker, 2003; Hassanzadeh et al., 2008; Ustaömer et al., 2009, 2011, 2012; Jamshidi Badr et al., 2013).

The Cadomian terranes in Iran and Turkey are often thought to be fragments rifted away from the Arabian–Nubian Shield (ANS). The ANS is dominated by Neoproterozoic crust formed between 900 and 580 Ma through the accretion of intra-oceanic arcs, leading to the closure of the Mozambique Ocean in the Cryogenian (e.g., the ocean between the Afif block and Sahara) and the amalgamation of Gondwana (Stern, 1994a,b, 2002; Johnson and Woldehaimanot, 2003; Collins and Pisarevsky, 2005; Stern, 2008; Stern and Johnson, 2010; Ali et al., 2013; Fritz et al., 2013). But the ocean was still open in the east in the Ediacaran (e.g., Collins and Pisarevsky, 2005; Johnson et al., 2011). The ANS records ~300 m.y. of orogenic evolution from intra-oceanic subduction, arc and back-arc magmatism (870–700 Ma), through terrane amalgamation (~800 to 650 Ma), to terminal collision between major fragments of eastern and western Gondwana, with attendant tectonic escape, strike-slip faulting, delamination, and extension (630–550 Ma) of

\* Corresponding author.

E-mail address: [hadishafaii@du.ac.ir](mailto:hadishafaii@du.ac.ir) (H. Shafaii Moghadam).

the newly formed continental crust (Kröner et al., 1987; Stern, 1994a,b; Genna et al., 2002; Johnson and Woldehaimanot, 2003; Avigad and Gvirtzman, 2009; Stern and Johnson, 2010; Johnson et al., 2011; Ali et al., 2013). However, the Cadomian basement is somewhat younger than the youngest ANS igneous rocks.

The overall uniformity of Ediacaran and Paleozoic platform strata that covered Central Iran and the Alborz provinces led to the notion that these regions were once part of an undivided Paleozoic Arabian–Iranian platform of the Gondwana supercontinent (e.g., Stöcklin, 1968, 1974). By analogy to the Arabian Shield and platform, continental crust of Neoproterozoic age was believed to underlie both Alborz and central Iran. Geochronological evidence tying Greek, Turkish as well as Iranian basements to the northern active margin of Gondwana came from Robertson and Dixon (1984), Şengör (1984), Ramezani and Tucker (2003), Hassanzadeh et al. (2008), Ustaömer et al. (2009, 2011) and Jamshidi Badr et al. (2013). Many of these basement terranes preserve evidence of latest Ediacaran–Early Cambrian magmatism (e.g., Ustaömer et al., 2009; Jamshidi Badr et al., 2013). In this scenario, Ediacaran–Early Cambrian magmatism is suggested to have formed a widespread continental active arc along the northern margin of Gondwana (e.g., Ramezani and Tucker, 2003; Hassanzadeh et al., 2008; Ustaömer et al., 2009, 2011).

In this paper we present new field data, whole rock major, trace, rare earth elements and Sr–Nd isotope geochemistry, U–Pb zircon dates and zircon Hf isotopic compositions to better understand the age and nature of metamorphic basement (granitic–tonalitic orthogneisses and associated amphibolites and paragneissic rocks) of the ChahJam (Torud)–Biarjmand metamorphic complex. We then use whole rock Nd and zircon Hf isotopes to infer the sources of these orthogneissic rocks. We are searching for the oldest basement rocks in central Iranian block and intend to relate these units to other dispersed Gondwanan continental fragments in Iran, Turkey and Afghanistan.

## 2. Geological setting

### 2.1. General view

The tectonic framework of Iran is made up of a number of Gondwana-derived micro-continents sutured together by ophiolitic remnants of Paleo-Tethys and Neo-Tethys oceanic lithosphere (Shafaii Moghadam and Stern, 2011). The continental blocks collided with Eurasia when Paleo-Tethys closed during Triassic time, generating a suite of collision-related granitoids of Late Triassic age in northeastern Iran (Karimpour et al., 2010). Collision with the most recent Gondwana fragment – Arabia – continues along the Bitlis–Zagros suture zone, part of the Zagros Orogenic Belt. This belt extends SE from eastern Turkey through northern Iraq and SW Iran to the Straits of Hormuz and into northern Oman, accommodating ~20 mm/yr of convergence between Arabia and Eurasia (Reilinger et al., 2006).

Iran can be divided into 8 major tectonic zones (Fig. 1), from N to S: 1) The Kopet–Dagh zone in NE Iran, which is part of the 500 km long and 100 km wide Turan block of Eurasia. 2) The Alborz zone in NW Iran, which is a ~600 km long and ~100 km wide belt of Precambrian to Recent magmatic and sedimentary rocks. 3) The Central Iranian block or microcontinent, consisting of three major crustal blocks (from E to W): Lut, Tabas, and Yazd (e.g., Alavi, 1991). These are the Cadomian blocks that drifted from Gondwana and accreted to Eurasia as the result of northward subduction and closure of Paleotethys in Permo-Triassic time (e.g., Berberian and King, 1981; Şengör, 1987; Stampfli, 2000). The Central Iran block includes sutures marked by Paleozoic (Jandagh–Anarak), and Late Cretaceous (Nain–Baft; Sabzevar) ophiolites. 4) The Eastern Iranian suture zone, between the Lut block in the west and the Afghan block in the east. The tectonic evolution of this zone was dominated by the emplacement of the Cretaceous Birjand–Nehbandan–Tchehel–Kureh ophiolites followed by deposition of Late Cretaceous–Paleocene flysch. 5) The Urumieh–Dokhtar magmatic belt, a 50–80 km

wide Andean-type magmatic belt of intrusive and extrusive rocks formed by northeastward subduction of Neo-Tethys beneath Iran during Late Cretaceous and Cenozoic time (Falcon, 1974; Berberian and Berberian, 1981; Berberian and King, 1981; Berberian et al., 1982; Alavi, 1994; Shahabpour, 2007; Chiu et al., 2013). 6) The Zagros Fold-Thrust Belt (ZFTB), an external (trench-ward) deformed part of the Zagros Orogen (Alavi, 1980, 1991, 1994). The Zagros Fold-Thrust Belt extends southeast for nearly 2000 km from southeastern Turkey through northern Syria and northeastern Iraq to western and southern Iran (Alavi, 1994). 7) The Sanandaj–Sirjan Zone (SSNZ), the metamorphic core of the Zagros orogen (Mohajjel et al., 2003) separating the inner and outer Zagros ophiolite belts. The Sanandaj–Sirjan Zone rocks span most of Phanerozoic time, including imbricated slices of marine and continental siliciclastic sediments metamorphosed under low- and medium-grade greenschist conditions (Alavi, 1994). 8) The Makran zone comprising Cretaceous ophiolitic units and younger flysch-type sediments, including Eocene to Miocene turbidites.

The metamorphic basement of Central Iran is considered to be Precambrian and is overlain by rare remnants of Paleozoic platform sediments. Mesozoic and Cenozoic sedimentary successions also cover the metamorphic basement. The metamorphic basement of the Central Iranian block is dominated by granitic to tonalitic gneiss, from which Ediacaran–Cambrian ages have been reported (Fig. 1; Ramezani and Tucker, 2003). This basement has been recognized in the Yazd–Tabas blocks, including a pocket of high-grade metamorphic rocks in the Chapedony–Saghand area (Fig. 1) interpreted to be a metamorphic core complex (Ramezani and Tucker, 2003; Verdel et al., 2007; Kargaranbafghi et al., 2012a). This basement was exhumed during Eocene crustal extension followed by Early Miocene erosion (Kargaranbafghi et al., 2012b). Ediacaran–Cambrian basement also occurs in other places in Iran (Fig. 1), including the Takab–Zanjan (Hassanzadeh et al., 2008), Soursat (Jamshidi Badr et al., 2013), and Khoy (Azizi et al., 2011) areas in NW Iran, and around Birjand in NE Iran. Ediacaran–Cambrian rocks also occur in the Alborz (Lahijan pluton) and in the Sanandaj–Sirjan Zone (Muteh region) (Hassanzadeh et al., 2008). In this paper we focus on the late Neoproterozoic–Cambrian basement in the Torud (ChahJam)–Biarjmand region in NE Iran (Fig. 1).

### 2.2. Geology of the ChahJam–Biarjmand complex

The ChahJam–Biarjmand complex (CJBC) covers >5000 km<sup>2</sup> and is flanked by the Alborz mountains in the north and the Lut–Tabas block to the south. The region between the Lut–Tabas blocks and the ChahJam–Biarjmand complex is a large desert and playa, composed of clay and salt deposits, which obscures the contact between the Saghand and Taknar metamorphic complexes to the south with the ChahJam–Biarjmand complex. To the north, the ChahJam–Biarjmand complex is surrounded by Eocene (Shafaii Moghadam, 2014; U–Pb zircon ages) volcanic and plutonic rocks of the Torud magmatic belt and by metamorphosed (phyllite, schist, marble) Paleozoic strata. Hushmandzadeh et al. (1978) considered the ChahJam–Biarjmand metamorphic rocks to be Precambrian. This was revised by a U–Pb zircon age of ~520 Ma for crystallization of the ChahJam orthogneisses (Rahmati-Ilkhchi et al., 2009). Ar–Ar and K–Ar ages on muscovite and biotite grains from ChahJam metagranites have yielded ages of ca. 160 and 171 Ma, respectively (Rahmati-Ilkhchi et al., 2009). These ages may record cooling after metamorphism of these metagranites.

The ChahJam region contains amphibolite-facies meta-igneous rocks and mica schist, and lower-grade Permian to Miocene cover sequences. These rocks were affected by four major deformation phases including Precambrian to Mid-Jurassic deformation, Cretaceous folding and Neogene folding (Rahmati-Ilkhchi et al., 2010). Lower-greenschist facies metamorphosed Jurassic sandstones and shales unconformably overlie the ChahJam–Biarjmand metamorphic basement, indicating that uplift and erosion occurred after Cadomian igneous activity and

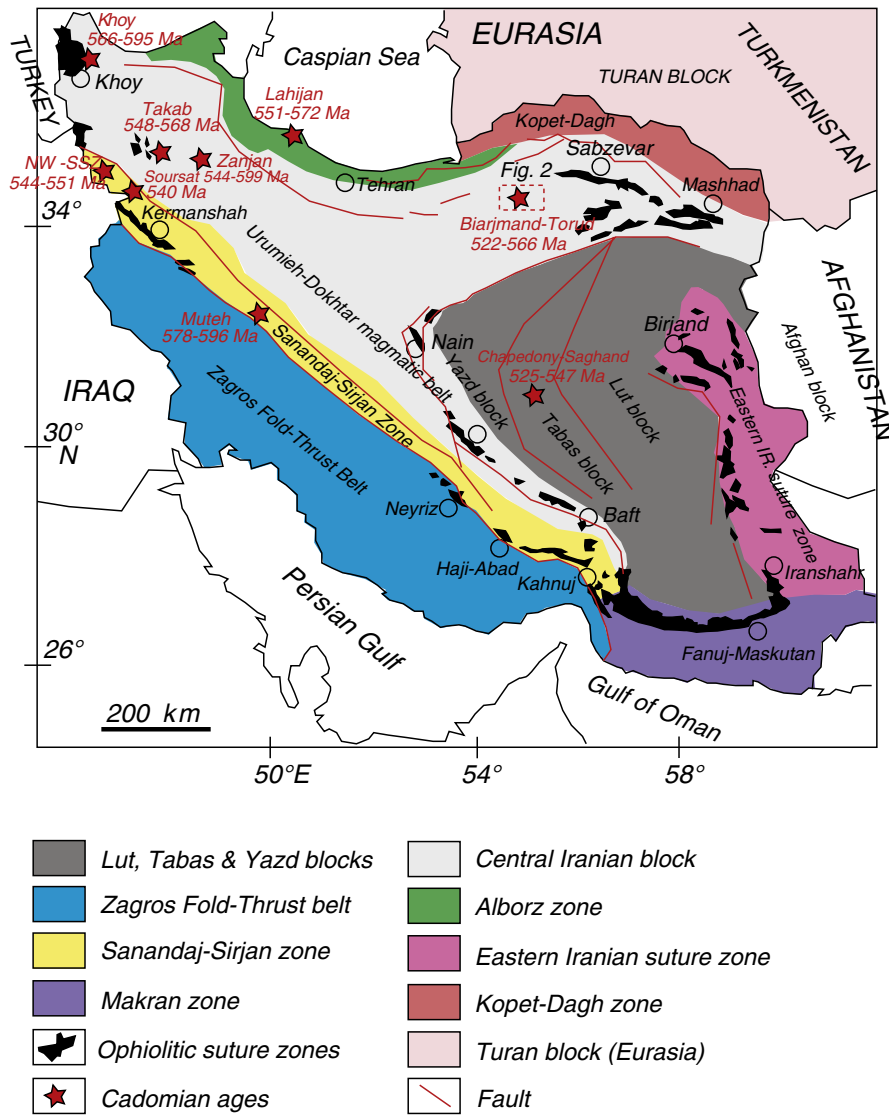


**Fig. 1.** Simplified geological map of Iran highlighting areas where Ediacaran–Cambrian (–600–520 Ma) radiometric ages are documented (stars) and the main ophiolitic belts (thick dashed lines). Numbers show U–Pb zircon ages (the age of the Soursat complex is from Jamshidi Badr et al., 2013; Khoy is from Azizi et al., 2011; other ages are from Hassanzadeh et al., 2008).

deformation and before Jurassic time. Jurassic strata are stratigraphically overlain by Jurassic–Cretaceous limestones of Kuh-e-Molhedou. As these units are separated from the Biarjmand metamorphic core by two major low-angle faults, a core complex model was suggested by Hassanzadeh et al. (2008).

The ChahJam metamorphic basement is divided into psammitic to volcanogenic meta-sediments (paragneiss, mica schist, garnet–mica schist and amphibolite), and orthogneiss consisting of meta-igneous felsic plutonic rocks and metamorphosed felsic and rare mafic (amphibolite) dikes and sills. There was no constraint on the age of deposition of the mica schists and other meta-sediments in this region. Orthogneiss (granitic protolith) intrudes the metasedimentary rocks. Orthogneissic granitic dikes are especially common around granitic–tonalitic orthogneissic plutons and intrude mica schist, amphibolites and meta-sediments. Some of these dikes contain tourmaline as elongated phenocrysts. Garnet-rich granitic mylonites with a quartz and feldspar (and biotite) stretching lineation are also abundant in the ChahJam region. Garnet-rich mylonitic leuco-granites occur as small plutons, crosscutting the whole ChahJam metamorphic sequence. Evidence of contact metamorphism is revealed by mica-rich veins and also by hornfels containing olivine, iron-rich cordierite, greenish hercynite, wollastonite

and tremolite. Augen gneiss is rare in the ChahJam region but becomes increasingly common toward Biarjmand. The alternation of felsic paragneiss (with quartz and feldspar), dark amphibolitic and even mica schist layers is common in the ChahJam region (in macroscopic and mesoscopic scale), probably representing protolith layering ( $S_0 = N40W, 10NE$ ) (Fig. 3A). The garnet mica schists are mineralogically similar to mica-rich paragneisses. Paragneissic rocks are mostly represented by alternating quartzo-feldspathic and foliated biotite-rich layers (Fig. 3B). Paragneisses, amphibolites and garnet–mica schists occasionally show deformed and folded quartzo-feldspathic bands/layers with scarce amphiboles, probably reflecting partial melting of the host rocks (Fig. 3C). The sequence exhibits strong ductile deformation with folding and development of LS-tectonites. Dark-green amphibolitic layers in the ChahJam–Biarjmand complex are up to several meters thick but they decrease in importance toward the Biarjmand region. These layers usually taper until they disappear. Metamorphosed aplitic to pegmatitic dikes are common in the ChahJam–Biarjmand orthogneisses.

In the Biarjmand region, fine-grained schists with marble intercalations are common. Coarse-grained augen orthogneiss (with large K-feldspar porphyroblasts) associated with slightly metamorphosed

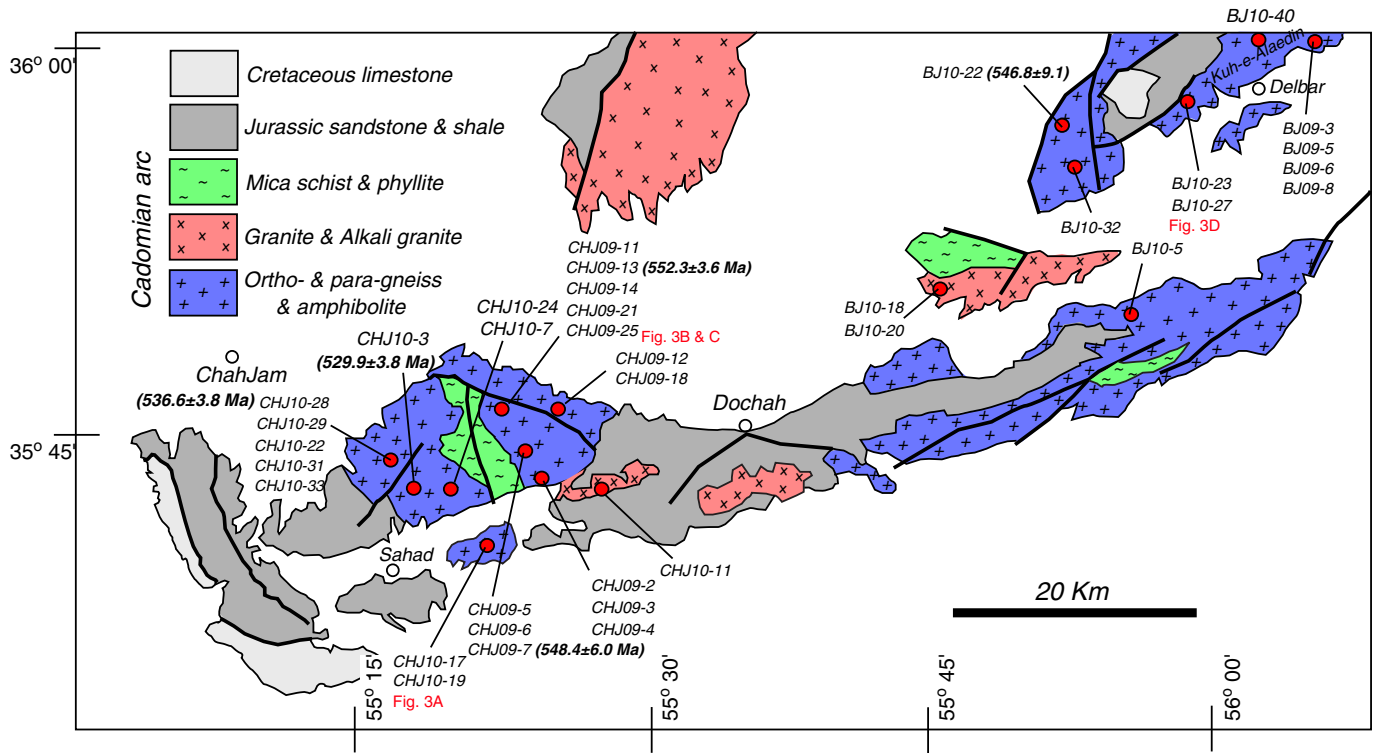


Fig. 2. Simplified geological map of the ChahJam–Birajmand metamorphic complex. Modified after 1/250,000 maps of Kharturan and Torud, Geological Survey of Iran.

A-type granitic to dioritic and even gabbroic plutons are abundant. Individual lenses or layers (a few meters thick) of greenish dark amphibolites are common in the Biarjmand orthogneisses but pinch out laterally. These amphibolites could represent attenuated mafic dikes or sills. Para-amphibolites with volcanogenic protoliths occur in the region, and host clinopyroxene-bearing (usually attenuated) coarse to fine-grained granitic dikes (Fig. 3D). High temperature andalusite-

sillimanite-bearing and/or high-pressure kyanite-bearing metapelitic rocks are rare. Orthogneisses are crosscut by younger (Eocene?) dark-green diabasic to plagioclase porphyritic basaltic dikes (~0.5–1 m thick). Younger diabasic dikes (~2 m thick) are abundant in the Kuh-e-Alaedin, making up a dike swarm complex (~N55E, 65SE av. for dikes). Erosional remnants of Eocene lavas occasionally cover the high-grade basement in the Biarjmand region. Large plutons of granite

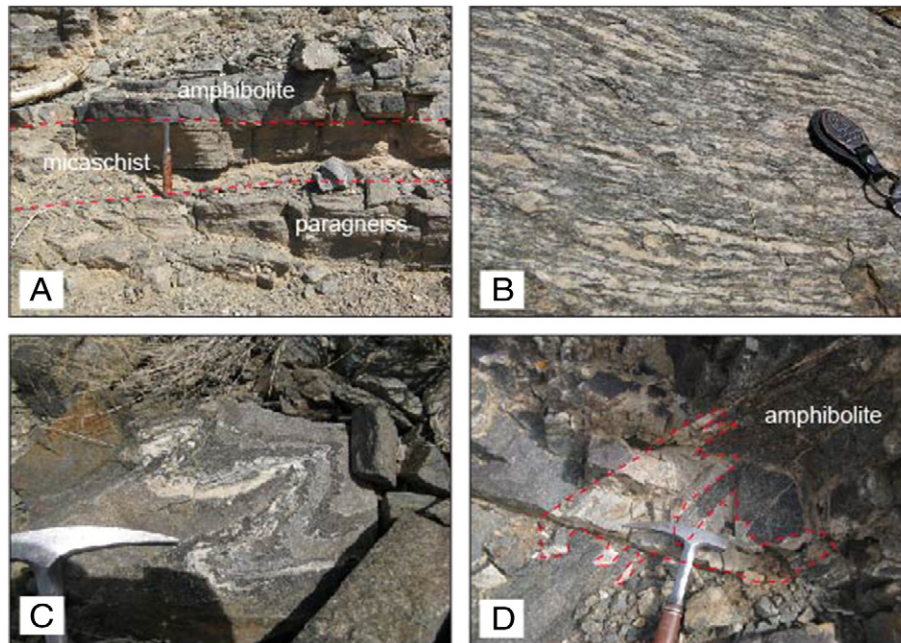


Fig. 3. Field photographs of the ChahJam–Biarjmand metamorphic complex. A) Alternation of amphibolite, mica schist and paragneiss in ChahJam region. B) Alternation of quartz-feldspathic and foliated biotite-rich layers in paragneiss. C) Quartzo-feldspathic folded layer with amphiboles in ChahJam complex. D) Intrusive contact of the attenuated metagranitic dike with host amphibolite in Biarjmand.

and alkali granite are common in the ChahJam–Biarjmand metamorphic complex (Fig. 2). These rocks also have Cadomian ages (U–Pb age ~ 520 Ma) and represent melts formed from lower crustal rocks at a convergent plate margin (Shafaii Moghadam et al., 2014).

**3. Petrography of ChahJam–Biarjmand metamorphic rocks**

This study focuses on the ChahJam–Biarjmand felsic igneous rocks, which share many geochemical characteristics. The metagranites and orthogneisses are compositionally similar but appear differently in the field. Metagranites show granular texture and contain mineral assemblages of alkali feldspar + plagioclase + quartz + biotite ± chlorite ± epidote ± sericite ± iron oxide. In the QAP diagram (Fig. 4A) after Streckeisen (1974), the ChahJam–Biarjmand metagranites (CHJ10-11; BJ10-18 and BJ10-20) plot predominantly in the field of monzogranite

and tonalite. Orthogneisses include mostly granitic gneisses but granodioritic and tonalitic gneisses are also common. Their mineral assemblages are quartz + orthoclase + plagioclase + microcline + biotite + garnet ± amphibole ± epidote ± allanite ± sphene ± zircon ± tourmaline ± iron oxides. In some leucogranitic gneisses, blue-green sodic amphiboles (riebeckite or barroisite) occur. Granitic to tonalitic gneisses show grano- to lepidoblastic texture defined by aligned biotite flakes. In the QAP diagram (Fig. 4A), the ChahJam–Biarjmand orthogneisses (CHJ09-7 (dated), -18, -21, -25; CHJ10-17, -24; BJ09-3, -6; BJ10-22 (dated), -23, -27) plot predominantly into the field of monzogranite and granodiorite except for one sample that plots within quartz diorite field.

Dikes within the orthogneiss and amphibolite (except younger diabasic dikes) vary from metagranitic to tonalitic (-gneissic) dikes. These dikes include quartz + alkali feldspar (orthoclase and

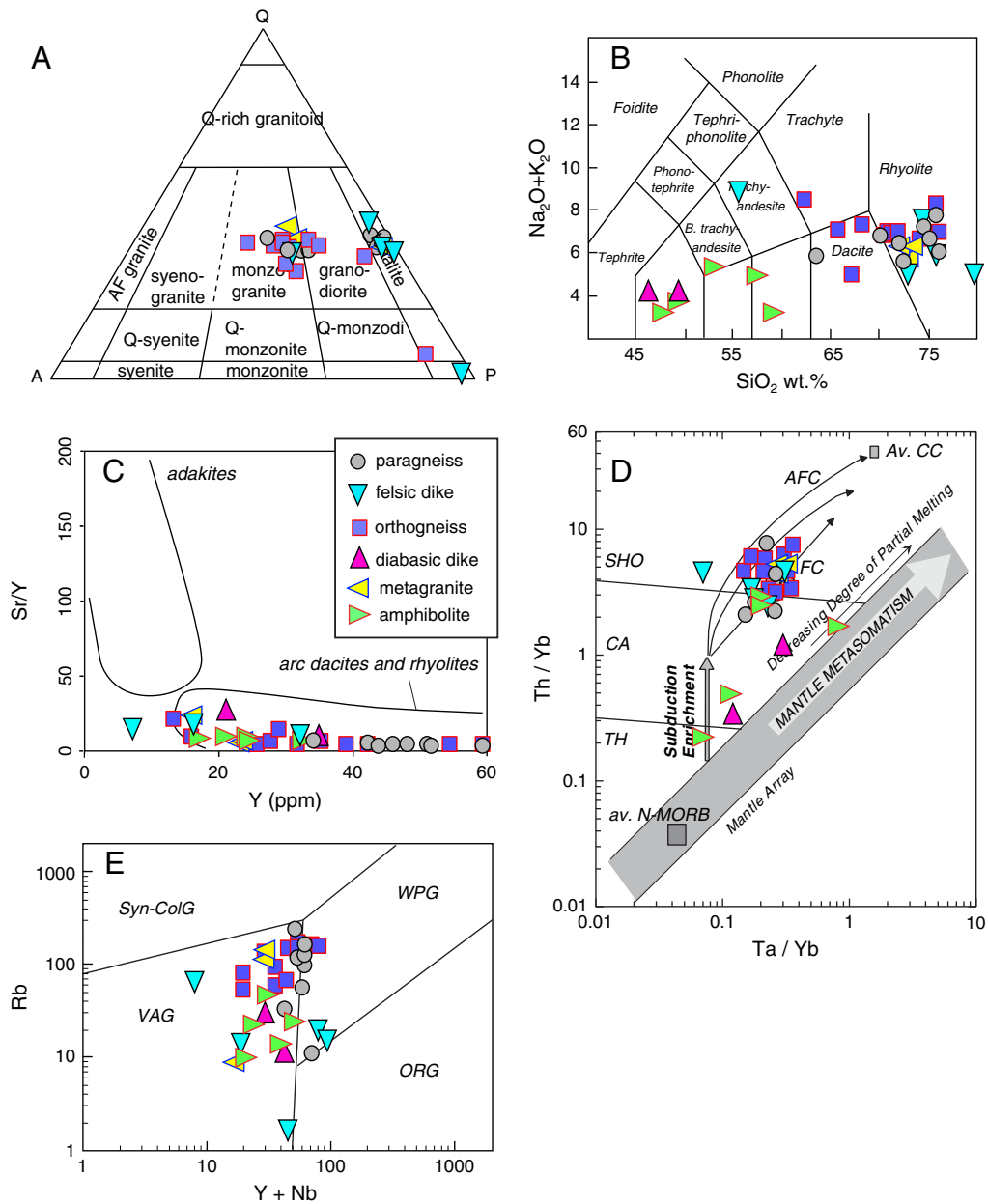


**Fig. 4.** A) QAP nomenclature diagram with normative mineral compositions. B) Total alkalis versus SiO<sub>2</sub> diagram for the ChahJam–Biarjmand rocks (after Le Bas et al., 1986). C) Sr/Y vs. Y diagram for discriminating adakites from arc dacites and rhyolites (the fields for adakite and normal island-arc dacites and rhyolites are based on the work of Defant and Drummond, 1990, 1993; Castillo et al., 1999). The ChahJam–Biarjmand rocks have low Sr/Y ratios similar to normal arc rocks. D) Th/Yb vs. Ta/Yb diagram (Pearce, 1982) showing ChahJam–Biarjmand rocks with high Th/Yb, reflecting contributions from subduction components and/or older continental crust. E) Rb vs. Y + Nb diagram (Pearce et al., 1984) for ChahJam–Biarjmand rocks.

microcline) + plagioclase + zircon ± garnet ± chlorite ± sphene ± biotite ± epidote ± muscovite ± tourmaline ± amphibole. Tiny amphiboles occur in some leucogranitic dikes intruding the amphibolites. Colorless to pale green clinopyroxenes were observed in a tonalitic gneissic dike (sample BJ10-40) within the orthogneiss. In the QAP diagram (Fig. 4A), the ChahJam–Biarjmand dikes (CHJ10-7, -19, -22, -33; BJ10-40) plot predominantly in the field of tonalite and diorite.

Paragneiss mineral assemblages include quartz + alkali feldspar + plagioclase + biotite ± garnet ± allanite ± sphene ± chlorite ± epidote ± muscovite ± zircon ± rutile (and normative corundum). Quartz grains show undulose extinction and sometimes show serrated contacts with neighboring quartz grains, especially in highly deformed quartz ribbons, suggesting grain boundary migration. Garnet occurs as large (>5 mm) to small crystals with inclusions of non-oriented quartz grains. The paragneiss metamorphic grade is lower to middle amphibolite facies.

Amphibolites contain hornblende or cummingtonite + plagioclase + quartz ± K-feldspar ± biotite ± chlorite ± sphene ± epidote ± garnet ± clinozoisite. Their metamorphic grade is middle amphibolite facies. Schists include fine-grained quartz, plagioclase, biotite and muscovite with tiny grains of epidote, clinozoisite and garnet. Young diabasic dikes contain sericitized plagioclase and clinopyroxene.

#### 4. Geochemistry of ChahJam–Biarjmand complex

Analytical methods and supplementary tables including ChahJam–Biarjmand whole rock analyses, Sr–Nd isotopes, U–Pb zircon dating, and zircon rare earth elements and Hf isotopes are available from the online version of the journal at: <http://dx.doi.org/10.1016/j.gr.2013.10.014>.

##### 4.1. Whole rock major and trace (rare earth) elements geochemistry

Representative whole rock analyses of the ChahJam–Biarjmand metamorphic rocks are presented in Supplementary Table 1 (available from the online version of the journal at: <http://dx.doi.org/10.1016/j.gr.2013.10.014>; locations are shown in Fig. 2).

Metagranites have quite uniform compositions with 72.7–73.8 wt.% SiO<sub>2</sub> and modest K<sub>2</sub>O (0.4–3.3 wt.%) and Na<sub>2</sub>O (3–5.3 wt.%) contents (Fig. 4B). The rocks have low Sr/Y, distinct from adakites and similar to normal arc rocks (Fig. 4C). Metagranites are represented by high Th/Yb values in Th/Yb vs. Ta/Yb diagrams (Pearce, 1982) (Fig. 4D), suggesting subduction-related enrichments and hence an arc source for these rocks. However contribution of continental crust during partial melting could also increase the Th/Yb ratio. In the Rb against Y + Nb diagram (Pearce et al., 1984), the metagranites show affinities to volcanic arc granites (VAG) but plot close the boundary with the “within-plate granite” field (Fig. 4E). These rocks have LREE-enriched patterns ( $La_{(n)}/Yb_{(n)} = 2.7–5.9$ ), and most show some Eu negative anomalies (except sample BJ10-11) (Fig. 5A). Enrichment in U, Th, Rb, Pb and depletion in Nb, Ta, and Ti relative to LREEs is conspicuous (Fig. 5B).

Orthogneissic rocks have tonalitic to granitic compositions with 62.2 to 76.2 wt.% SiO<sub>2</sub> (Supplementary Table 1; Fig. 4B). Their Na<sub>2</sub>O and K<sub>2</sub>O contents vary between 2.6–7.2 wt.% and 1.4–5.7 wt.%, respectively (Supplementary Table 1). These rocks also have low Sr/Y (Fig. 4C). Their Th/Yb is very high, similar to arc-related rocks, but this may reflect assimilation of continental crust during ascent (AFC trend) and/or simply derivation from partial melting of lower continental crust (Fig. 4D). Most rocks have volcanic arc granite (VAG) signatures in the Rb vs. Y + Nb diagram (Pearce et al., 1984), but some plot toward the within plate granite (WPG) field (Fig. 4E). These rocks have LREE enriched patterns from La to Sm but with relatively flat patterns from Tb to Lu (Fig. 5C). Their  $La_{(n)}/Yb_{(n)}$  ratio varies from 3.2 to 31.2 (Supplementary Table 1). The nature of the negative Eu anomalies suggests that the rocks evolved by fractional crystallization of plagioclase or that they originated from partial melting in the presence of

feldspar in the source. Positive anomalies in Rb, Ba, U, Th and negative anomalies in Nb, Ta, Sr and Ti relative to LREEs are the main characteristics of these rocks (Fig. 5D). Enrichment in Large Ion Lithophile Elements (LILEs) and depletion in High Field Strength Elements (HFSEs) suggest that these rocks originated above a subduction zone. Depletion in Ti and Sr could be related to the titanomagnetite and feldspar (with Eu anomaly) fractionation.

Dikes intruding orthogneisses and meta-granites have 72.9 to 79.9 wt.% SiO<sub>2</sub> with granitic compositions in the TAS (Total Alkalies versus Silica) diagram (Fig. 4B), except sample CHJ10-7 (55.4%), which has a relatively high LOI content (~6%). Dikes have low Sr/Y but very high Th/Yb abundances, further denoting an arc or older continental source. In the Rb vs. Nb + Y diagram (Pearce et al., 1984), samples show volcanic arc granite signatures except for two samples that have within-plate granite affinity. Within plate (WPG) signatures for some metagranitic dikes and orthogneisses denote high Y (& Nb) concentrations (Supplementary Table 1), and are related to the presence of garnet in these rocks (confirmed with petrographical evidences). Dikes have variable  $La_{(n)}/Yb_{(n)}$  ratios (0.6–9.6) with high HREE contents, further indicating garnet influence. Depletion in Ti and Nb and enrichment in U, Th and Pb relative to LREEs are other characteristics of the metagranitic dikes.

Paragneissic rocks have 63.7 to 76.2 wt.% SiO<sub>2</sub> and resemble the orthogneissic rocks in the TAS diagram (Fig. 4B). These rocks also have elevated Th/Yb (Fig. 4D). The rocks have quite similar REE patterns with LREE enrichment relative to HREEs ( $La_{(n)}/Yb_{(n)} = 4.1–7.2$ ) (Fig. 5E) and negative Eu anomalies. Similar to the orthogneisses, these rocks are also characterized by positive anomalies in Rb, Th, U, Pb and negative anomalies in Nb, Ti and Sr, suggesting arc-related meta-sedimentary protoliths.

Amphibolites have mafic compositions, with between 47.4 and 58.8 wt.% SiO<sub>2</sub>. These rocks have variable Th/Yb ratios, but mostly plot far from a mantle array trend (Fig. 4D). Amphibolites have flat to LREE fractionated patterns ( $La_{(n)}/Yb_{(n)} = 1.1–8.8$ ) (Fig. 5G). Variable depletion in Nb and enrichment in LILEs relative to LREEs are characteristics of the amphibolites (Fig. 5H). These features are consistent with arc tholeiitic and calc-alkaline signatures for these rocks.

Diabasic dikes have basaltic compositions (46–49 wt.% SiO<sub>2</sub>) and display arc signatures with quite high Th/Yb (Fig. 4D). Enrichment in LREE/HREE associated with positive anomalies in Ba, U, Th, Pb and negative anomalies in Nb relative to LREEs also indicates a calc-alkaline affinity for the diabasic dikes.

##### 4.2. Sr–Nd isotopes

Sr–Nd isotope analyses of the ChahJam–Biarjmand gneissic rocks are presented in Supplementary Table 2 (available from the online version of the journal at: <http://dx.doi.org/10.1016/j.gr.2013.10.014>). <sup>87</sup>Rb/<sup>86</sup>Sr range widely, low (<1) for felsic dike samples but high (>2) for metagranite, granite gneiss, and paragneiss. As a result, correction for radiogenic growth (assumed to be 550 Ma) gives initial <sup>87</sup>Sr/<sup>86</sup>Sr of varying reliability. The initial <sup>87</sup>Sr/<sup>86</sup>Sr of both granitic (gneissic) rocks and paragneisses calculated at 550 Ma range between 0.6803 and 0.7461, but most have elevated values of 0.7056 and 0.7168 (Supplementary Table 2). Paragneissic rocks and metagranitic dikes have similarly elevated initial <sup>87</sup>Sr/<sup>86</sup>Sr (Fig. 6). Samples with low <sup>87</sup>Rb/<sup>86</sup>Sr provide the most reliable initial <sup>87</sup>Sr/<sup>86</sup>Sr. The three felsic dike samples with <sup>87</sup>Rb/<sup>86</sup>Sr < 1 give initial <sup>87</sup>Sr/<sup>86</sup>Sr = 0.7087 to 0.7461. Moderate to high <sup>87</sup>Sr/<sup>86</sup>Sr for the gneissic rocks (samples BJ10-22 and CHJ10-22 respectively) suggests involvement of older crust.

The εNd (550) values of orthogneisses, metagranites and dikes range from –2.2 to –5.5, indicating that older continental crust was remelted to generate the granitic magmas. These values are similar to that (εNd –1.2 to –2.9) of Cadomian metagranites from the Bitlis massif (Turkey) (Ustaömer et al., 2009). Paragneisses have similar εNd values, ranging between ~–3 and –3.7 (Supplementary Table 2).

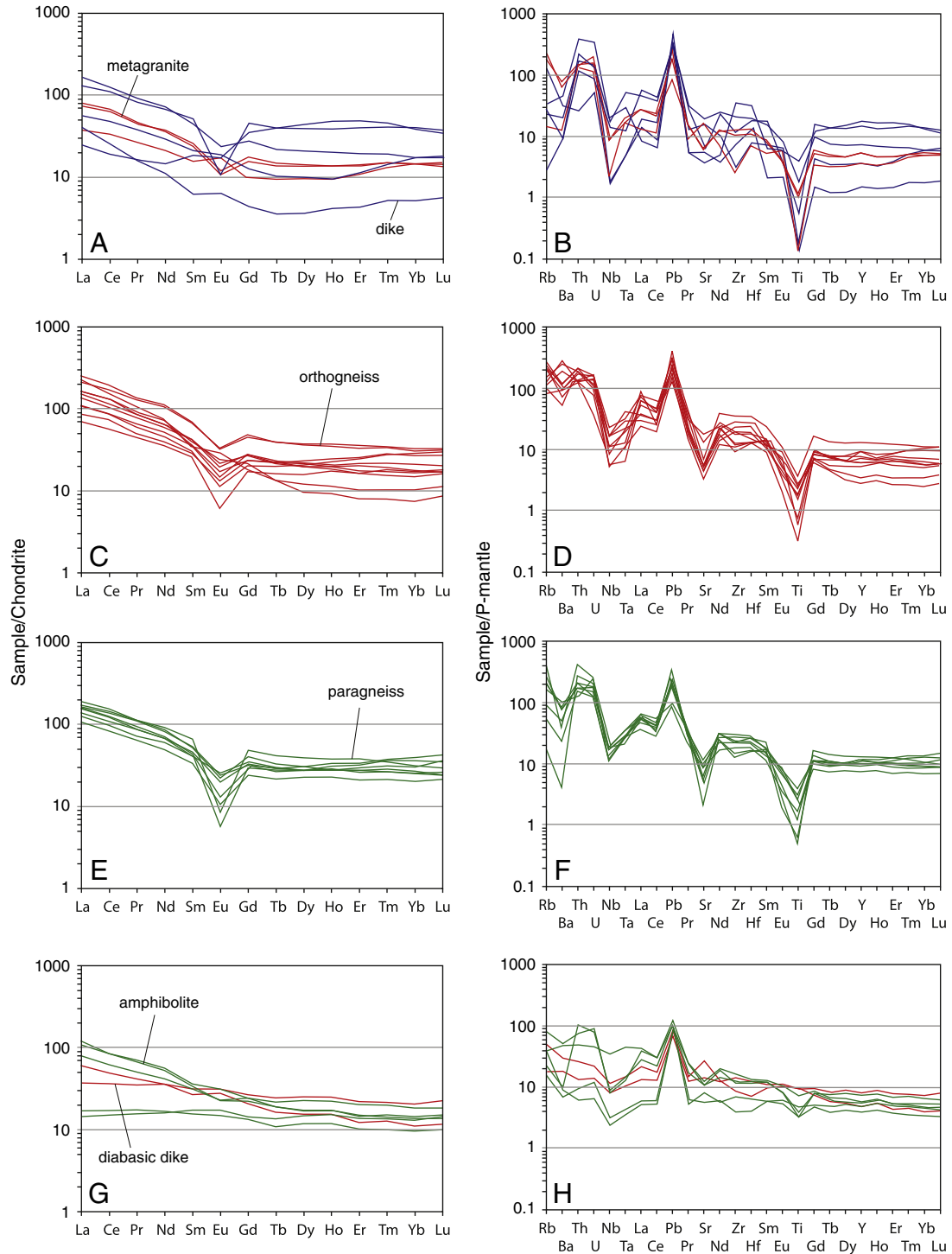


Fig. 5. Chondrite-normalized rare earth element and trace elements patterns for the ChahJam–Biarjmand rocks.

$^{143}\text{Sm}/^{144}\text{Nd}$  is low for all samples, 0.117 to 0.151, so meaningful Nd model ages ( $T_{\text{DM}}$ ) can be calculated.  $T_{\text{DM}}$  model ages cluster tightly around 1.35 to 1.65 Ga (Supplementary Table 2).

## 5. Zircon U–Pb dating, REE, and Hf isotopic compositions

Five samples from the ChahJam–Biarjmand complex were selected for U–Pb zircon dating and Hf-isotopic analysis of zircons: four granitic gneiss samples and one sample of paragneiss. Locations of dated samples are shown in Fig. 2 and results for each of the five samples are discussed below.

### 5.1. U–Pb zircon dating

#### 5.1.1. Sample BJ10-22 (granitic gneiss)

The zircon crystals have short prismatic (rarely long) shapes. In CL images, most grains are euhedral and zoned (Fig. 7). Core and rim structures are rare. A total of 18 spot analyses were carried out on this sample (Supplementary Table 3). The analyses show large variations in U contents of 177–1907 ppm and Th contents of 67–985 ppm, resulting in variable Th/U ratios of 0.18–0.81. This high Th/U ratio (>0.1) is consistent with an igneous origin for the analyzed zircons.  $^{206}\text{Pb}/^{238}\text{U}$  ages range from ~645 to 532 Ma (Supplementary Table 3).

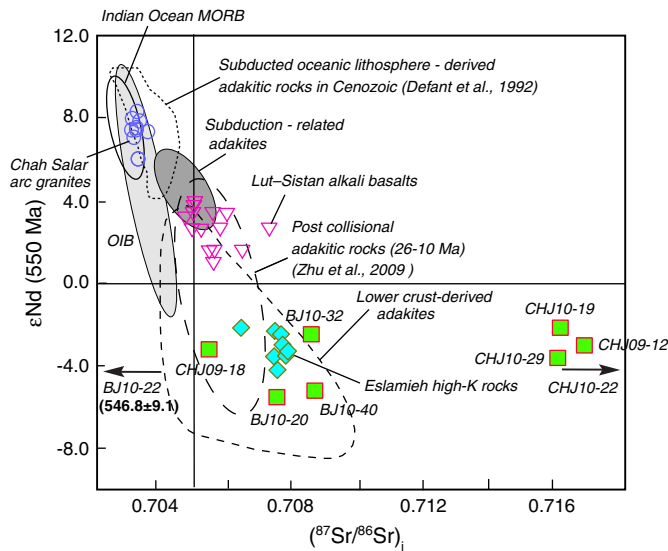


**Fig. 6.** Initial  $\epsilon_{\text{Nd}}$  vs.  $^{87}\text{Sr}/^{86}\text{Sr}$  for the ChahJam–Biarjmand rocks compared with subduction-related, lower crust-derived (Defant et al., 1992) and post-collisional adakites (Zhou et al., 2009). Data for Lut–Sistan alkali basalts are from Pang et al. (2012), for Chah Salar arc granites from Shafaii Moghadam et al. (2014), and Eslamieh high-K rocks from Shafaii Moghadam et al. (2014).

On a concordia diagram (Fig. 8), most analyses are slightly or moderately discordant. The analyses have a weighted mean  $^{206}\text{Pb}/^{238}\text{U}$  age of  $546.8 \pm 9.1$  Ma (MSWD of concordance = 2.6) (Fig. 8), interpreted the time of zircon crystallization. These zircons have fractionated HREE patterns, positive Ce and negative Eu anomalies (Fig. 9), probably indicating that they formed in equilibrium with feldspar (Wang et al., 2010). These patterns further suggest that the zircons are of igneous origin.

#### 5.1.2. Sample CHJ10-28 (granitic gneiss)

Zircons in this sample are prismatic, euhedral and/or subhedral (to oval-like). In CL images, some grains have core-rim structures but magmatic zoning is rare. The zircons show variable U (121–611 ppm) and Th contents (61–290 ppm) (Supplementary Table 3) with Th/U ratios varying from 0.18 to 0.82. The  $^{206}\text{Pb}/^{238}\text{U}$  ages of zircons range from 648 to 496 Ma (Supplementary Table 3). Most analyses are concordant with mean  $^{206}\text{Pb}/^{238}\text{U}$  age of  $536.6 \pm 3.8$  Ma (MSWD = 0.88) (Fig. 8), although some analyses are discordant. The older ages (ca. 646 Ma) are interpreted as being inherited xenocrysts. In a chondrite-normalized REE diagram, the zircons show positive Ce and moderate negative Eu anomalies, but have steep HREE patterns (Fig. 9), consistent with their igneous origin (Rubatto, 2002; Wu and Zheng, 2004).

#### 5.1.3. Sample CHJ09-7 (granitic gneiss)

Zircons are euhedral to subhedral (and even oval-shape) and short (and rarely long)-prismatic. In CL images, zircons are rarely translucent and most are dark. Some grains have core-rim structures. A few zircons have oscillatory zoning, suggesting an igneous origin (Wu et al., 2007; Buick et al., 2008). Zircons have high U (159–4982 ppm) and Th contents (53–1089 ppm), and moderately high Th/U ratios (0.11–0.68), except for two grains with low Th/U (0.05 & 0.08) (Supplementary Table 3).  $^{206}\text{Pb}/^{238}\text{U}$  ages range from 1097 to 462 Ma (Supplementary Table 3). Younger ages (ca. 462 Ma) belong to zircons with low Th/U. Analyses older than 562 Ma are interpreted as being inherited xenocrysts. Most analyses are concordant (Fig. 8), yielding a  $^{206}\text{Pb}/^{238}\text{U}$  age of  $548.4 \pm 6.0$  Ma (MSWD of concordance = 1.6). This age is interpreted to reflect the crystallization age of the granitic protolith. The zircons show steep HREE patterns, positive Ce anomalies and prominent negative Eu anomalies (Fig. 9), consistent with their crystallization from a melt (Rubatto, 2002; Rubatto et al., 2009).

#### 5.1.4. Sample CHJ10-3 (granitic gneiss)

Zircons in sample CHJ10-3 are 100 to 200  $\mu\text{m}$  long and prismatic (Fig. 7). They show oscillatory zoning in CL images. The zircons have moderate contents of U (180–702 ppm) and Th (84–417 ppm) (except one grain with 1013 ppm U and 667 ppm Th) with Th/U varying from 0.31 to 0.83 (Supplementary Table 3). Most analyses are concordant, yielding a  $^{206}\text{Pb}/^{238}\text{U}$  age of  $529.9 \pm 3.8$  Ma (Fig. 8). The analyses that lie to the right of concordia are interpreted to reflect common lead and/or lead loss. Their  $^{207}\text{Pb}/^{206}\text{Pb}$  ages vary between ca. 509 and 1428 Ma. The old ages are associated with high U (or Th) zircons and/or are related to inherited cores. The zircons have steep HREE patterns with positive Ce and negative Eu anomalies (Fig. 9), consistent with their igneous origin (Rubatto, 2002; Wu and Zheng, 2004).

#### 5.1.5. Sample CHJ09-13 (paragneiss)

In CL images, most zircon grains show oval to short-long prismatic shapes, and a few show core-rim structures (Fig. 7). Some grains show oscillatory zoning, whereas others are sector-zoned or unzoned (Fig. 7), suggesting that they may have been derived from different sources. The zircons show large variations in U contents (205 to 1653 ppm) and Th (51–470 ppm), with Th/U of 0.18–0.69. This moderately high Th/U is consistent with a magmatic origin. The zircons have steep HREE patterns (except one old zircon with a flat HREE trend), positive Ce and moderate negative Eu anomalies (Fig. 9). The  $^{206}\text{Pb}/^{238}\text{U}$  ages of the zircons range from 2397 to 420 Ma (Supplementary Table 3). Four zircon grains (points 1 & 17) have old  $^{207}\text{Pb}/^{206}\text{Pb}$  ages of 2457 and 1732 Ma as well as younger ages of 609–620 Ma (points 7, 12 & 18, points on rim) reflecting re-worked grains. Most analyses plot on concordia yielding a  $^{206}\text{Pb}/^{238}\text{U}$  age of  $552.3 \pm 3.6$  Ma (MSWD of concordance = 0.37) (Fig. 8). This age is similar to the ages obtained from the orthogneissic rocks (ca. 548 Ma for sample CHJ09-7 and 530 Ma for sample CHJ10-3), suggesting that the sedimentary protolith of the paragneiss was deposited between ~552 and ~530 Ma. This suggests that the Andean arc, presumably the source of detrital zircons in the sedimentary protolith of the paragneiss, was close to the sedimentary basin. Younger  $^{206}\text{Pb}/^{238}\text{U}$  concordant ages of ca. 502 and 483 Ma are possibly metamorphic ages.

## 5.2. Zircon Hf isotopes

The initial Hf-isotope ratios ( $(^{176}\text{Hf}/^{177}\text{Hf})_{\text{initial}}$ ) for the ChahJam–Biarjmand gneissic rocks (Supplementary Table 5) range from 0.281276 to 0.282590 with negative to slightly positive  $\epsilon_{\text{Hf}}(t)$  of  $-7.03$  to  $+3.33$  (except one point with  $\epsilon_{\text{Hf}}(t) = 7.81$ ) (Fig. 10), suggesting involvement of older continental crust in magma genesis. This is consistent with bulk rock  $\epsilon_{\text{Nd}}(t)$  values.  $T_{\text{DM1}}$  age is the single-stage model age of Hf-isotopes assuming that the sample was derived from depleted mantle, whereas  $T_{\text{DM2}}$  is a two-stage model age of Hf-isotopes via the lower crust following derivation from depleted mantle. The samples show a  $T_{\text{DM1}}$  of 919–1292 Ma and a  $T_{\text{DM2}}$  of 1083–1753 Ma (except two points with old U–Pb ages). We consider only  $T_{\text{DM2}}$  to have geological meaning, because it is consistent with Sr and Nd isotopic evidence for involvement of older crust and the presence of old zircons in the ChahJam–Biarjmand paragneiss.

## 6. Discussion

### 6.1. Interpretation of age and geochemical data

The ChahJam–Biarjmand metamorphic rocks include paragneiss, amphibolite, mica schist and orthogneiss. These rocks were metamorphosed at lower amphibolite facies, presumably in the middle crust. The granitic to tonalitic orthogneisses have I-type signatures with trace and rare earth element characteristics similar to arc-related granites. They have high Rb and low Nb + Y contents similar to volcanic arc granites (VAG), except some samples with higher modal garnet and

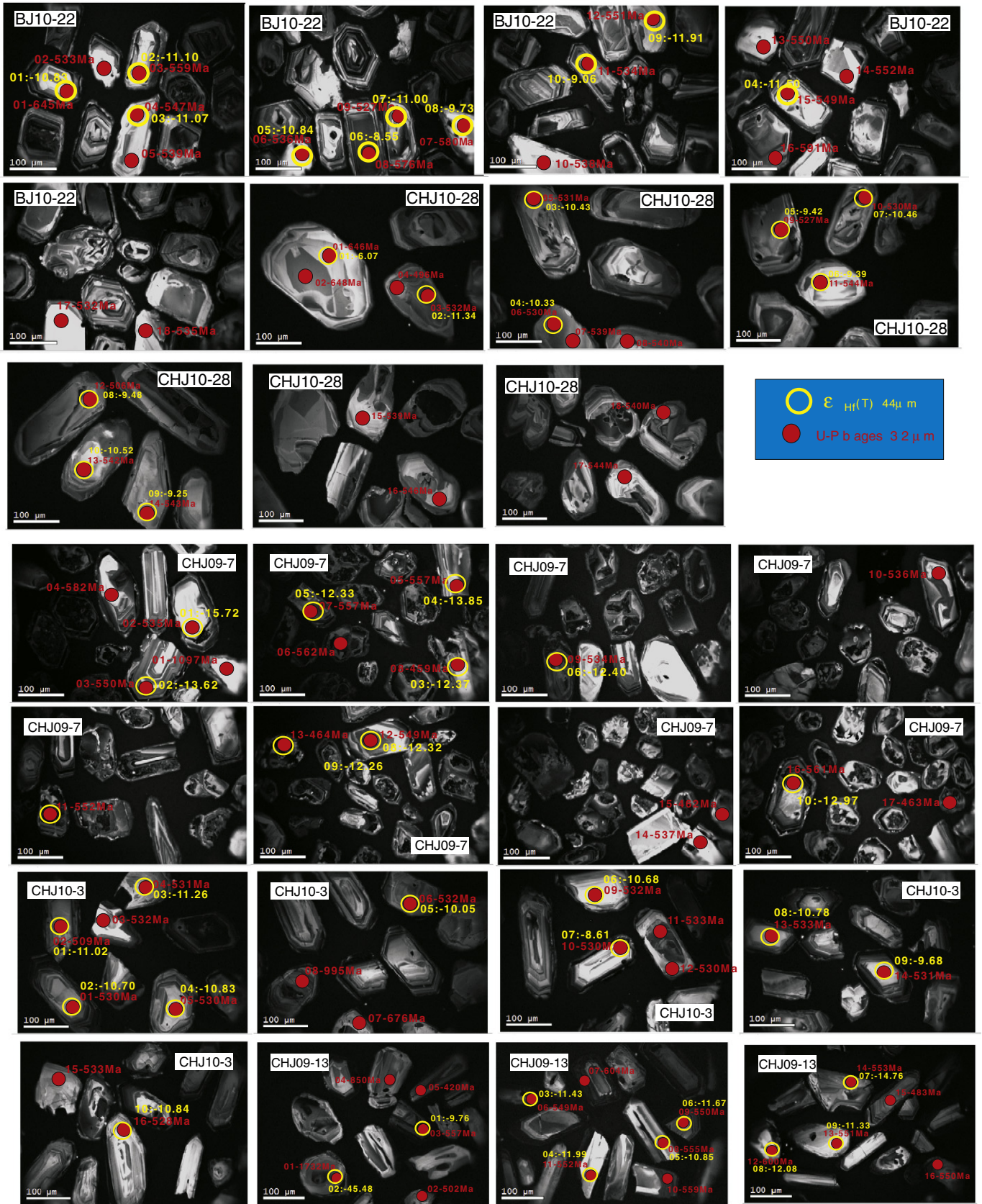


Fig. 7. Cathodoluminescence (CL) images and laser ablation ages for zircons from the ChahJam–Biarjmand gneissic rocks (large yellow dot denotes spot for Hf analysis, small red dot is laser spot).

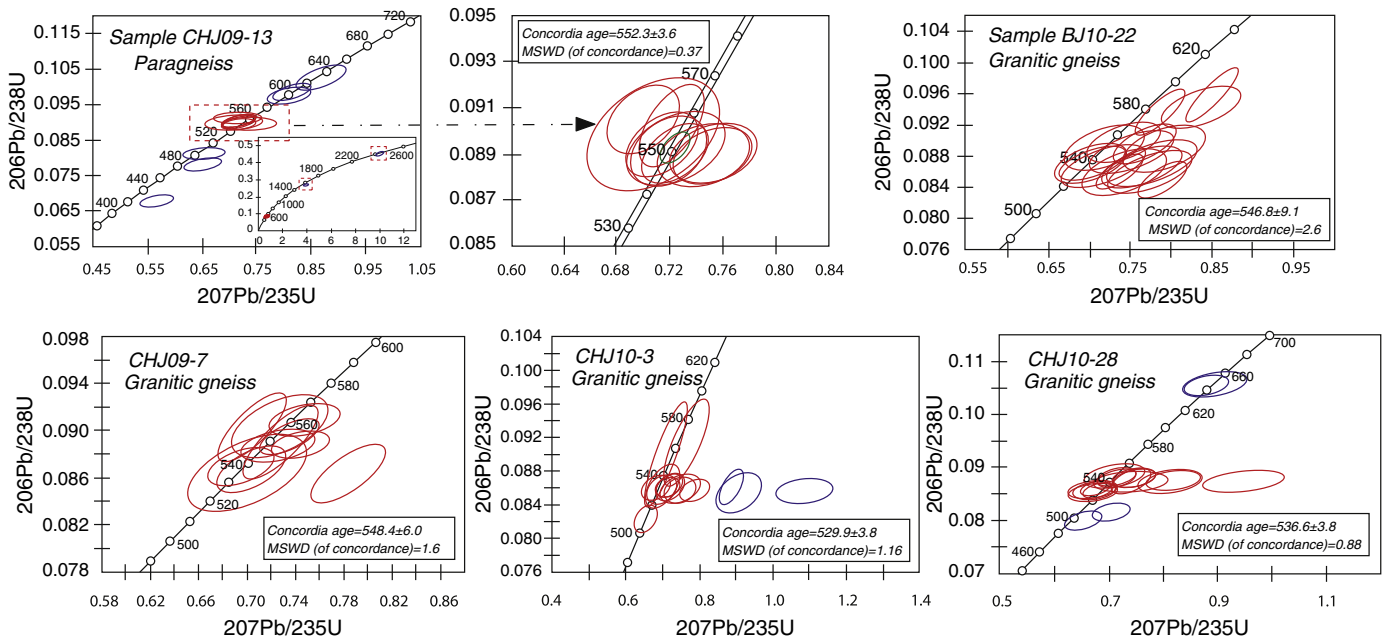


Fig. 8. U–Pb concordia plots of zircon ages for ChahJam–Biarjmand gneissic rocks.

biotite that show within-plate granite (WPG) signatures. The general sense is that The ChahJam–Biarjmand metamorphic complex represents the roots (middle crust) of an Andean-type arc. Biotite could have controlled Nb enrichment while garnet has influenced Y abundance. Paragneiss with high modal biotite also displays enriched Nb contents. Amphibolites have tholeiitic to calc-alkaline characteristics and their geochemical signature suggests a supra-subduction zone tectonic setting. Orthogneisses have broadly similar  $^{206}\text{Pb}/^{238}\text{U}$  ages from ca. 530 to 548 Ma. It seems that magmatic activity lasted only around 18 m.y. Detrital zircon from paragneiss yielded old  $^{207}\text{Pb}/^{206}\text{Pb}$  ages of 2457

and 1732 Ma as well as younger ages of 609–620 Ma, but most populations have  $^{206}\text{Pb}/^{238}\text{U}$  ages of 552 Ma. It seems that the clastic fill of the sedimentary basin was shed from a local source area, dominated by Ediacaran–Cambrian igneous rocks with minor clastic materials coming from older strata and/or igneous rocks. Variable but high Sr isotopic compositions of granitic to tonalitic gneisses and dikes along with negative  $\varepsilon\text{Nd}$  (–2.2 to –5.5) implicate older continental crust; Nd and Hf model ages suggest that this older crust is Mesoproterozoic, ~1.5 Ga. These results together with zircon Hf isotopes are interpreted to mean that the rocks reflect partial melting of Mesoproterozoic continental crust.

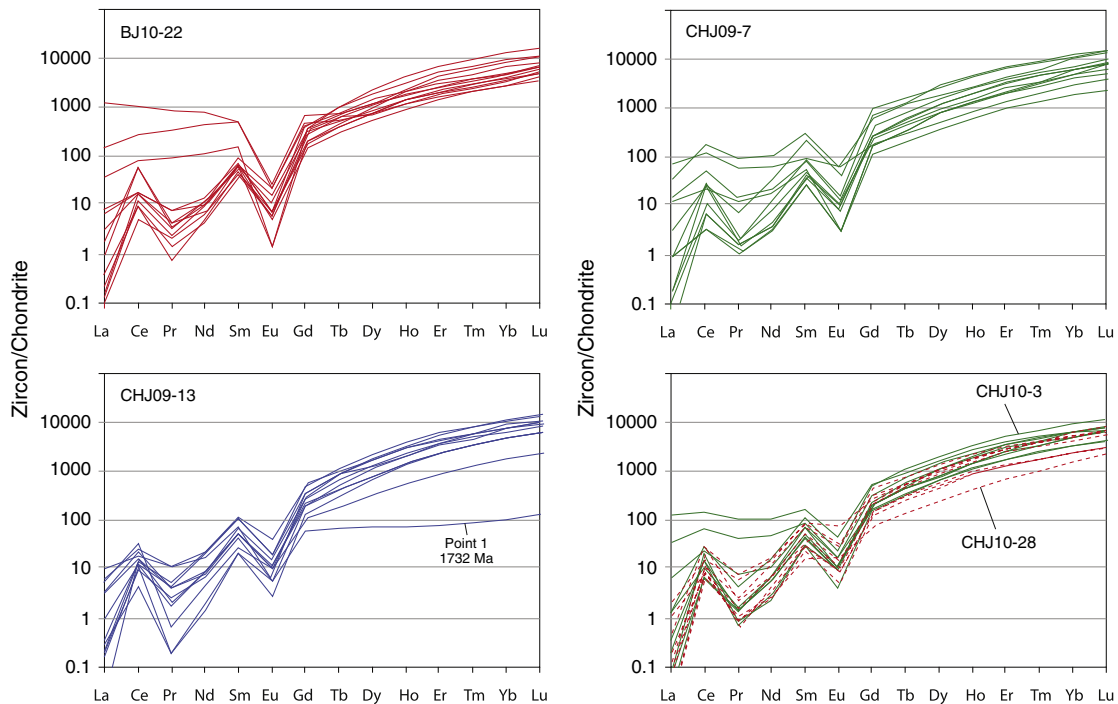


Fig. 9. Chondrite-normalized REE patterns of zircon in samples from the ChahJam–Biarjmand complex. Chondrite-normalize values are from Sun and McDonough (1989).

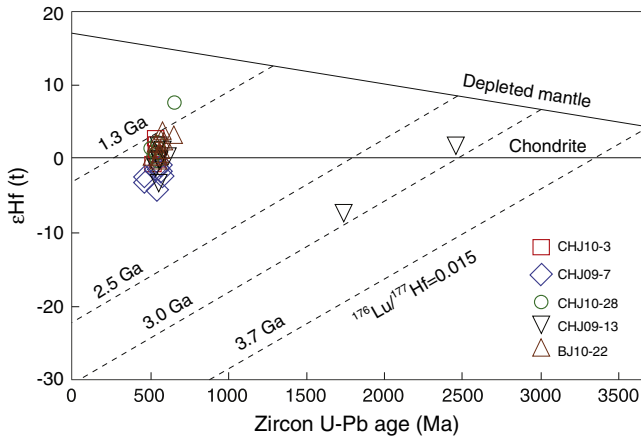


Fig. 10. U–Pb age vs.  $\epsilon_{\text{Hf}}$  for zircons from the ChahJam–Biarjmand gneissic rocks.

6.2. Mesoproterozoic crust in Iran?

All zircon ages for basement rocks of Iran reported to date are Ediacaran–Cambrian. Our Sr, Nd and Hf isotopic studies of CJB gneisses indicate that these may not be juvenile additions to the crust from the mantle, but contain a significant admixture of older continental crust. Nd and Hf model ages suggest that this older continental crust was Mesoproterozoic (1000–1600 Ma), but so far no reliable ages older than 600 Ma have been reported for any Iranian rock (Fig. 11). It is difficult to unequivocally interpret the significance of these model ages, but it seems likely that older Proterozoic and even Archean basement may exist in Iran or at least in areas attached to Iranian terranes at that time. However, these older model ages could be from sedimentary rocks derived from older Proterozoic or even Achaean sources (and not necessarily directly from Mesoproterozoic igneous sources), as would

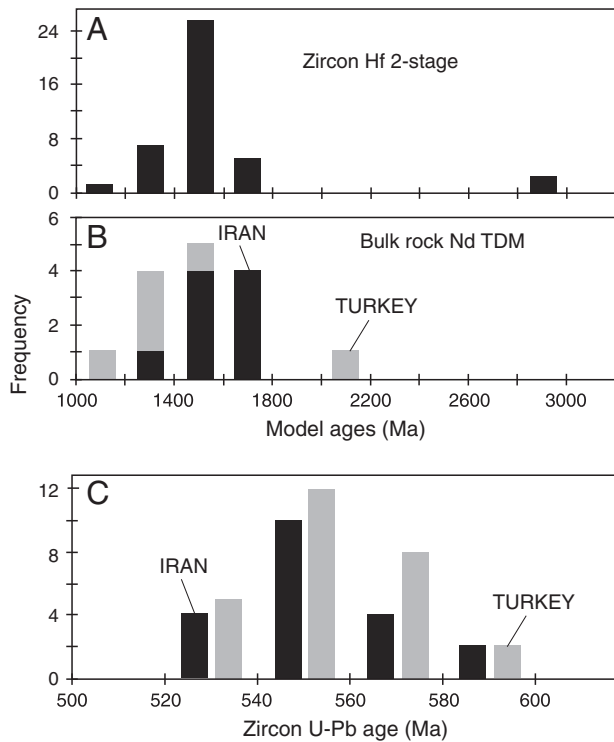


Fig. 11. Histograms showing U–Pb zircon age distributions, Nd model ages and zircon Hf model ages for Ediacaran–Cambrian basements in Iran and Turkey. Data on Iran are similar to Fig. 1. Nd model age data are from Ustaömer et al. (2009, 2011) and U–Pb zircon ages for Turkey are from Yilmaz Sahin et al. (2014).

be the case if the Andean arc was formed on an inverted passive margin with sediments in the passive margin derived from older terranes. Further geochronological and isotopic studies of Ediacaran–Cambrian basement units in Iran are needed to address this question. Similarities in the isotopic and geochronological record reported from SE Turkey (Ustaömer et al., 2009, 2012) suggest that the Iranian terranes stretched into what is now Turkey (Fig. 11).

6.3. Geodynamic implications

Gondwana was assembled by the collision of about 7–8 Australia-sized Neoproterozoic continents mainly during two periods: 1) at ~650–600 Ma and 2) at ~570–520 Ma (Collins and Pisarevsky, 2005; Ustaömer et al., 2009). After final amalgamation of Gondwana, an Andean-type active margin formed along the Australia–Antarctica and South America sector of the Gondwana as well as northern margin of the India (Foden et al., 2006; Cawood et al., 2007) (Fig. 12). This type of margin also can be traced westward into Central Iran (ca. 599–525 Ma) (Ramezani and Tucker, 2003; Hassanzadeh et al., 2008; this study), the Sanandaj–Sirjan Zone (ca. 596–540 Ma) (Hassanzadeh et al., 2008; Jamshidi Badr et al., 2013), the Alborz (~551–572 Ma) and then into Turkey, mainly in the Tauride–Anatolian platform (570–540 Ma, Gürsu et al., 2004; Gessner et al., 2004; Gürsu and Göncüoğlu, 2006), the Istanbul fragment (Bolu massif, 576–565 Ma, Chen et al., 2002; Ustaömer et al., 2005), the Armutlu metagranites (565–585 Ma, Okay et al., 2008), and the Bitlis massif of SE Turkey (545–531 Ma; Ustaömer et al., 2009 and 572 Ma, Ustaömer et al., 2012).

The Cadomian–Avalonian fragments rifted from the north Gondwana margin during the Cambrian–Ordovician and accreted to Laurasia at various times (Nance et al., 2008, 2010). In the case of Iran, Cadomian fragments (sometimes called Cimmeria) accreted to Eurasia in Triassic times (Şengör and Natalin, 1996). The early Paleozoic cover strata are missing in the ChahJam–Biarjmand metamorphic complex and Jurassic sediments are the youngest strata that stratigraphically overlie the ChahJam–Biarjmand metamorphic complex.

The subduction of Iapetus oceanic lithosphere during Ediacaran–Cambrian time was responsible for arc magmatism in northern Gondwana (Fig. 12). This period of igneous activity was also an important crust-forming episode for Turkey (Gürsu and Göncüoğlu, 2005, 2006) and SW and central Europe (D’Lemos et al., 1990; Dörr et al., 2002; Genna et al., 2002; Murphy et al., 2002; Mushkin et al., 2003). To the south, the Arabian–Nubian Shield shows older magmatic activity, starting from at least ~900 Ma (Johnson et al., 2011; Ali et al., 2013). Subduction beneath the active margin of Gondwana is suggested to have ceased around 450–400 Ma, due to continental or oceanic plateau collision (Ustaömer et al., 2009) and/or to the change in relative plate motion. After this collision, early Ordovician to Silurian rifting opened Paleotethys (Fig. 12), separating slices of N Gondwana including the Istanbul fragment (Bolu massif, Ustaömer et al., 2005) from the southern basement fragments. The evidence of this rifting in NE Iran includes the Soltan–Meidan basalts and Ordovician (~460 Ma; Shafaii Moghadam et al., 2014) alkaline shallow plutons/sills. Further rifting of Gondwana’s northern margin in Permian times (~280–250 Ma) and Neotethys propagation was responsible for the separation of central Iran, the Alborz and the Tauride–Anatolian blocks and their travel toward Eurasia, each containing Cadomian rocks. These terranes again re-amalgamated to the Arabian Plate in Oligo–Miocene times.

The ChahJam–Biarjmand orthogneisses and metagranites have negative  $\epsilon_{\text{Nd}}$  (bulk rock) and negative to slightly positive zircon  $\epsilon_{\text{Hf}}$ , suggesting that these granites were not direct melts from either subducted oceanic lithosphere or the mantle wedge. Instead they come from partial melting of lower continental crust. Pooling of mantle-derived mafic magmas could be responsible for partial melting of continental lithosphere along the northern Gondwana active margin. Alternatively, a three step model was suggested for the Ediacaran–Cambrian arc rocks in Turkey (Gürsu and Göncüoğlu, 2005), including:

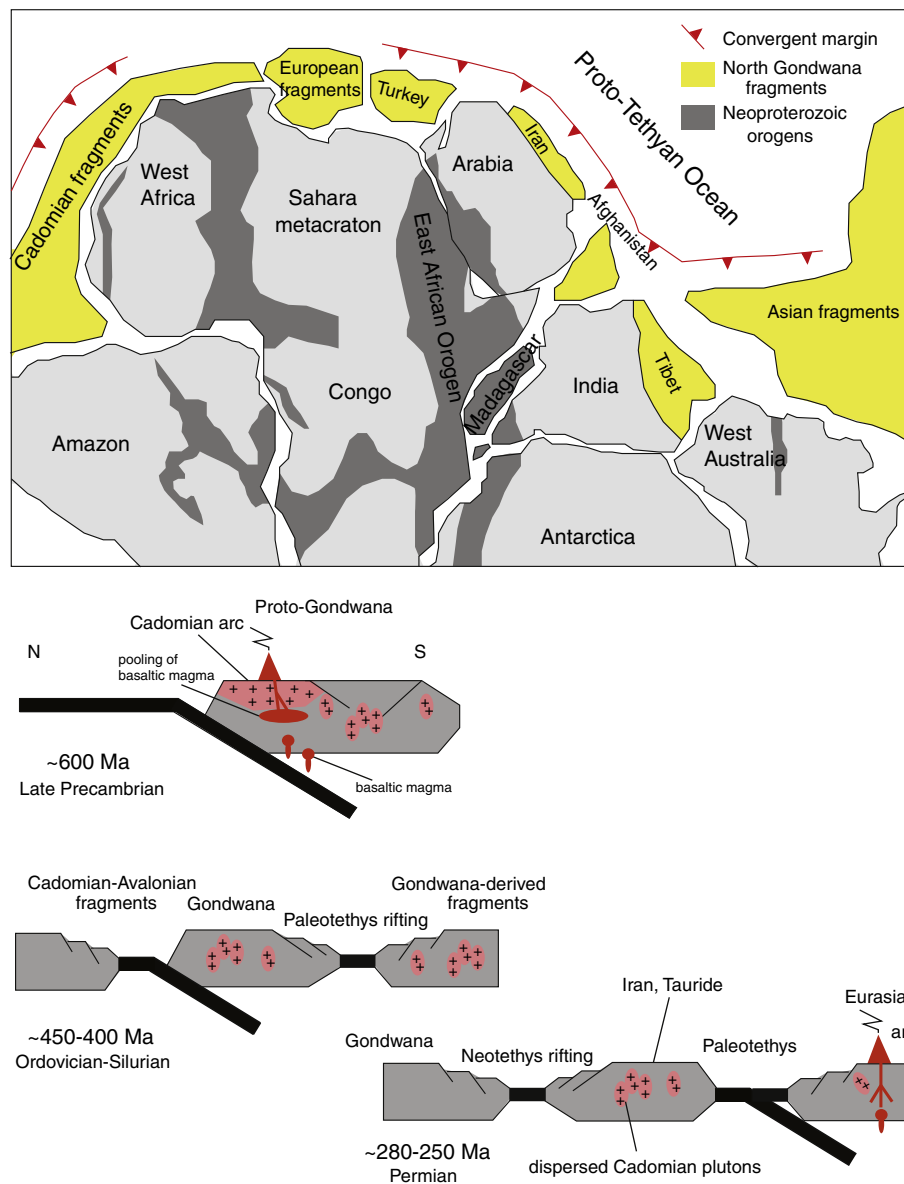


**Fig. 12.** Map of a part of Gondwana, showing the position of the continents and smaller continental fragments in the early Mesozoic. Summary of the tectonic evolution of Cadomian terranes within Iran and Turkey is shown in a series of panels (see text for explanations). Modified after Stern, 1994a,b.

(i) the injection of arc magmas into Gondwana basement above a southward-subducting northern margin of Gondwana at ca. 590–570 Ma, (ii) initial stages of extension and rifting within Gondwana continental crust and the formation of I-type granites (with post-collisional/extensional geochemical signature) at ca. 550–540 Ma, and (iii) lithospheric thinning and back-arc extension within the Gondwana pericratonic margin above the southward subducting system during the early Cambrian (ca. 540–530 Ma). The latter phase was accompanied by eruption of spilitic lavas and diabasic dikes in the Sandikli region (Turkey) with back-arc basin geochemical characteristics. The second stage of model, proposed by Gürsu and Göncüoğlu (2005), is supported here for the generation of the continental crust-derived ChahJam–Biarjmand Ediacaran–Cambrian granites.

## 7. Conclusions

Metagranites, orthogneisses and paragneissic rocks of the ChahJam–Biarjmand metamorphic complex have late Neoproterozoic (Ediacaran)

to early Cambrian ages, and are further evidence for a pulse of Cadomian magmatism at the northern active margin of Gondwana. Geochemical data show that the rocks formed in a subduction-related tectonic setting via partial melting of lower continental crust. Paleogeographically, the ChahJam–Biarjmand complex together with other similar age basements in Central Iran, the Sanandaj–Sirjan region, the Alborz block (Iran), and the Tauride–Anatolian block (Turkey) were part of Gondwana until later in the Paleozoic, when they separated during Neotethys rifting and were re-amalgamated in Oligo-Miocene times.

Supplementary data to this article can be found online at <http://dx.doi.org/10.1016/j.gr.2013.10.014>.

## Acknowledgments

Financial support from the Research Council of Damghan University with the Grant number 88/Geo/74/140 is acknowledged. We are very grateful to P. Ayda Ustaömer and Alan Collins for their constructive

reviews of the manuscript. Editorial suggestions by Prof. R. Damian Nance are highly appreciated.

## References

- Alavi, M., 1980. Tectonostratigraphic evolution of the Zagrosides of Iran. *Geology* 8, 144–149.
- Alavi, M., 1991. Sedimentary and structural characteristics of the Paleo-Tethys remnants in northeastern Iran. *Geological Society of America Bulletin* 103, 983–992.
- Alavi, M., 1994. Tectonics of the Zagros orogenic belt of Iran: new data and interpretations. *Tectonophysics* 229, 211–238.
- Ali, K.A., Wilde, S.A., Stern, R.J., Moghazi, A.M., Ameen, S.M.M., 2013. Hf isotopic composition of single zircons from Neoproterozoic arc volcanics and post-collision granites, Eastern Desert of Egypt. Implications for crustal growth and recycling in the Arabian–Nubian Shield. *Precambrian Research*. <http://dx.doi.org/10.1016/j.precamres.2013.05.016>.
- Avigad, D., Gvirtzman, Z., 2009. Late Neoproterozoic rise and fall of the northern Arabian–Nubian Shield: the role of lithospheric mantle delamination and subsequent thermal subsidence. *Tectonophysics* 77, 217–228.
- Azizi, H., Chung, S.L., Tanaka, T., Asahara, Y., 2011. Isotopic dating of the Khoy metamorphic complex (KMC), northwestern Iran: a significant revision of the formation age and magma source. *Precambrian Research* 185, 87–94.
- Berberian, F., Berberian, M., 1981. Tectono-plutonic episodes in Iran, in Zagros, Hindu Kush, Himalaya. In: Gupta, H.K., Delany, F.M. (Eds.), *Geodynamic Evolution*. AGU, Washington, DC, pp. 5–32.
- Berberian, M., King, G.C.P., 1981. Towards a paleogeography and tectonic evolution of Iran. *Canadian Journal of Earth Sciences* 18, 210–265.
- Berberian, F., Muir, I.D., Pankhurst, R.J., Berberian, M., 1982. Late Cretaceous and early Miocene Andean-type plutonic activity in northern Makran and central Iran. *Journal of the Geological Society (London)* 139, 605–614.
- Buick, I.S., Storker, A., Williams, I.S., 2008. Timing relationships between pegmatite emplacement, metamorphism and deformation during the intra-plate Alice Springs Orogeny, central Australia. *Journal of Metamorphic Geology* 26, 915–936.
- Castillo, P.R., Janney, P.E., Solidum, R.U., 1999. Petrology and geochemistry of Camiguin Island, southern Philippines: insights to the source of adakites and other lavas in a complex arc setting. *Contributions to Mineralogy and Petrology* 134, 33–51.
- Cawood, P.A., Johnson, M.R.W., Nemchin, A.A., 2007. Early Palaeozoic orogenesis along the Indian margin of Gondwana. Tectonic response to Gondwana assembly. *Earth and Planetary Science Letters* 255, 1–2 (15, 70–84).
- Chen, F., Siebel, W., Satir, M., Terzioğlu, N., Saka, K., 2002. Geochronology of the Karadere basement (NW Turkey) and implications for the geological evolution of the Istanbul zone. *International Journal of Earth Sciences* 91, 469–481.
- Chiu, H.Y., Chung, S.L., Zarrinkoub, M., Mohammadi, S.S., Khatib, M.M., Iizuka, Y., 2013. Zircon U–Pb age constraints from Iran on the magmatic evolution related to Neotethyan subduction and Zagros orogeny. *Lithos* 162–163, 70–87.
- Collins, A.S., Pisarevsky, S.A., 2005. Amalgamating eastern Gondwana: the evolution of the circum-Indian orogens. *Earth-Science Reviews* 71, 229–270.
- D’Lemos, R.S., Strachan, R.A., Topley, C.G., 1990. The Cadomian orogeny in the North Armorican Massif: a brief review. In: D’Lemos, R.S., Strachan, R.A., Topley, C.G. (Eds.), *The Cadomian Orogeny*. Geological Society Special Publication, vol. 51, pp. 3–12.
- Defant, M., Drummond, M., 1990. Derivation of some modern arc magmas by melting of young subducted lithosphere. *Nature* 347, 662–665.
- Defant, M., Drummond, M., 1993. Mount Street Helens: potential example of the partial melting of the subducted lithosphere in a volcanic arc. *Geology* 21, 547–550.
- Defant, M.J., Jackson, T.E., Drummond, M.S., DeBoer, J.Z., Bellon, H., Feigenson, M.D., Maury, R.C., Stewart, R.H., 1992. The geochemistry of young volcanism throughout western Panama and southeastern Costa Rica: an overview. *Journal of the Geological Society (London)* 149, 569–579.
- Dörr, W., Zulauf, G., Fiala, J., Franke, W., Vejnar, Z., 2002. Neoproterozoic to Early Cambrian history of an active plate margin in the Tepla-Barrandian unit – a correlation of U–Pb isotopic dilution – TIMS ages (Bohemia, Czech Republic). *Tectonophysics* 352, 65–85.
- Falcon, N.L., 1974. Southern Iran: Zagros Mountains. In: Spencer, A.M. (Ed.), *Mesozoic–Cenozoic Orogenic Belts, Data for Orogenic Studies*. Geological Society of London, Special Publication, pp. 199–211.
- Fernández-Suárez, J., Gutiérrez-Alonso, G., Jenner, G.A., Tubrett, M.N., 2000. New ideas on the Proterozoic–Early Paleozoic evolution of NW Iberia: insights from U–Pb detrital zircon ages. *Precambrian Research* 102, 185–206.
- Fernández-Suárez, J., Gutiérrez-Alonso, G., Jeffries, T.E., 2002. The importance of along-margin terrane transport in northern Gondwana: insights from detrital zircon parentage in Neoproterozoic rocks from Iberia and Brittany. *Earth and Planetary Science Letters* 204, 75–88.
- Foden, J., Elburg, M.A., Dougherty-Page, J., Burt, A., 2006. The timing and duration of the Delemerian Orogeny: correlation with the Ross Orogen and implications for Gondwana assembly. *Journal of Geology* 114, 189–210.
- Fritz, H., Abdelsalam, M., Ali, K., Bingen, B., Collins, A.S., Fowler, A.R., Ghebreab, W., Hauzenberger, C.A., Johnson, P., Kusky, T., Macey, P., Muhongo, S., Stern, R.J., Viola, G., 2013. Orogen styles in the East African Orogens: a review of the Neoproterozoic to Cambrian tectonic evolution. *Journal of African Earth Sciences* 86, 65–106.
- Genna, A., Nehlig, P., Le Goff, E., Guerrot, C., Shanti, M., 2002. Proterozoic tectonism of the Arabian Shield. *Precambrian Research* 117, 21–40.
- Gessner, K., Collins, A.S., Ring, U., Güngör, T., 2004. Structural and thermal history of poly-orogenic basement: U–Pb geochronology of granitoid rocks in the southern Menderes Massif, Western Turkey. *Journal of the Geological Society* 161, 93–101.
- Griffin, W.L., Wang, X., Jackson, S.E., Pearson, N.J., O’Reilly, S.Y., Xu, X., Zhou, X., 2002. Zircon chemistry and magma mixing, SE China: in situ analysis of Hf isotopes, Tonglu and Pingtan igneous complexes. *Lithos* 61, 237–269.
- Gürsu, S., Gönçüoğlu, M.C., 2005. Early Cambrian back-arc volcanism in the Western Taurides, Turkey: implications for the rifting along northern Gondwanan margin. *Geological Magazine* 142 (5), 617–631.
- Gürsu, S., Gönçüoğlu, M.C., 2006. Petrogenesis and tectonic setting of Cadomian felsic igneous rocks, Sandikli area of the western Taurides, Turkey. *International Journal of Earth Sciences* 95, 741–757.
- Gürsu, S., Gönçüoğlu, M.C., Bayhan, H., 2004. Geology and geochemistry of the pre-Early Cambrian rocks in Sandikli area: implications for the Pan-African evolution in NW Gondwanaland. *Gondwana Research* 7 (4), 923–935.
- Hassanzadeh, J., Stockli, D.F., Horton, B.K., Axen, G.J., Stockli, L.D., Grove, M., Schmitt, A.K., Walker, J.D., 2008. U–Pb zircon geochronology of late Neoproterozoic–Early Cambrian granitoids in Iran: implications for paleogeography, magmatism, and exhumation history of Iranian basement. *Tectonophysics* 451, 71–96. <http://dx.doi.org/10.1016/j.tecto.2007.11.062>.
- Hushmandzadeh, A.R., Alavi Naini, M., Haghipour, A.A., 1978. Evolution of geological phenomenon in Totud area. *Geological Survey of Iran Report* H5. 136 p. (in Farsi).
- Jamshidi Badr, M., Collins, A.S., Masoudi, F., Cox, G., Mohajjel, M., 2013. The U–Pb age, geochemistry and tectonic significance of granitoids in the Soursat Complex, Northwest Iran. *Turkish Journal of Earth Sciences* 21. <http://dx.doi.org/10.3906/yer-1001-37>.
- Johnson, P.R., Woldehaimanot, B., 2003. Development of the Arabian–Nubian Shield: perspectives on accretion and deformation in the northern East African Orogen and the assembly of Gondwana. In: Yoshida, M., Windley, B.F., Dasgupta, S. (Eds.), *Proterozoic East Gondwana: Super Continent Assembly and Break-up*. Geological Society of London Special Publication, 206.
- Johnson, P.R., Andresen, A., Collins, A.S., Fowler, A.R., Fritz, H., Ghebreab, W., Kusky, T., Stern, R.J., 2011. Late Cryogenian–Ediacaran history of the Arabian–Nubian Shield: a review of depositional, plutonic, structural, and tectonic events in the closing stages of the northern East African Orogen. *Journal of African Earth Sciences* 61, 167–232.
- Kargaranbafghi, F., Foeken, J.P.T., Guest, B., Stuart, F.M., 2012a. Cooling history of the Chapedony metamorphic core complex, Central Iran: implications for the Eurasia–Arabia collision. *Tectonophysics* 524–525, 100–107.
- Kargaranbafghi, F., Neubauer, F., Genser, J., Faghih, A., Kusky, T., 2012b. Mesozoic to Eocene ductile deformation of western Central Iran: from Cimmerian collisional orogeny to Eocene exhumation. *Tectonophysics* 564–565, 83–100.
- Karimpour, M.H., Stern, C.R., Farmer, G.L., 2010. Zircon U–Pb geochronology, Sr–Nd isotope analyses, and petrogenetic study of the Dehnow diorite and Kuhsangi granodiorite (Paleo-Tethys), NE Iran. *Journal of Asian Earth Sciences* 37, 384–393.
- Kröner, A., Greiling, R.O., Reischmann, T., Hussein, I.M., Stern, R.J., Durr, S., Kruger, J., Zimmer, M., 1987. Pan African crustal evolution in northeast Africa. In: Kroner, A. (Ed.), *Proterozoic Lithospheric Evolution*. Am. Geophysical Union, Washington, DC, pp. 69–94.
- Le Bas, M.J., Le Maitre, R.W., Streckeisen, A., Zanettin, B.A., 1986. A chemical classification of volcanic rocks based on the total alkaline–silica diagram. *Journal of Petrology* 27, 745–750.
- Mohajjel, M., Fergusson, C.L., Sahandi, M.R., 2003. Cretaceous–Tertiary convergence and continental collision Sanandaj–Sirjan western Iran. *Journal of Asian Earth Sciences* 21, 397–412.
- Murphy, J.B., Eguiluz, L., Zulauf, G., 2002. Cadomian orogens, peri-Gondwanan correlatives and Laurentia–Baltica connections. *Tectonophysics* 352, 1–9.
- Murphy, J.B., Pisarevsky, S.A., Nance, R.D., Keppie, J.D., 2004. Neoproterozoic Early Paleozoic evolution of peri-Gondwanan terranes: implications for Laurentia–Gondwana connections. *International Journal of Earth Sciences* 93, 659–682.
- Mushkin, A., Navon, O., Halicz, L., Hartmann, G., Stein, M., 2003. The petrogenesis of A-type magmas from the Amram massif, Southern Israel. *Journal of Petrology* 44, 815–832.
- Nance, R.D., Murphy, J.B., Keppie, J.D., 2002. A Cordilleran model for the evolution of Avalonia. *Tectonophysics* 352, 11–31.
- Nance, R.D., Murphy, J.B., Strachan, R.A., Keppie, J.D., Gutiérrez-Alonso, G., Fernández-Suárez, J., Quesada, C., Linnemann, U., D’Lemos, R., Pisarevsky, S.A., 2008. Neoproterozoic–early Paleozoic tectonostratigraphy and palaeogeography of the peri-Gondwanan terranes: Amazonian v. West African connection. In: Ennih, N., Liégeois, J.-P. (Eds.), *The Boundaries of the West African Craton*. Geological Society of London Special Publication, vol. 297, pp. 345–383.
- Nance, R.D., Gutiérrez-Alonso, G., Keppie, J.D., Linnemann, U., Murphy, J.B., Quesada, C., Strachan, R.A., Woodcock, N., 2010. Evolution of the Rheic Ocean. *Gondwana Research* 17 (2–3), 194–222.
- Okay, A.I., Bozkurt, E., Satir, M., Yigitbas, E., Crowley, Q.G., Shang, C.K., 2008. Defining the southern margin of Avalonia in the Pontides: geochronological data from the Late Proterozoic and Ordovician granitoids from NW Turkey. *Tectonophysics* 461, 252–264.
- Pang, K.-N., Chung, S.-L., Zarrinkoub, M.H., Mohammadi, S.S., Yang, H.-M., Chu, C.-H., Lee, H.-Y., Lo, C.-H., 2012. Age, geochemical characteristics and petrogenesis of Late Cenozoic intraplate alkali basalts in the Lut-Sistan region, eastern Iran. *Chemical Geology* 306–307, 40–53.
- Pearce, J.A., 1982. Trace element characteristics of lavas from destructive plate boundaries. In: Thorpe, R.S. (Ed.), *Andesites*. Wiley, New York, pp. 525–548.
- Pearce, J.A., Harris, N.B.W., Tindle, A.G., 1984. Trace element discrimination diagrams for the tectonic interpretation of granitic rocks. *Journal of Petrology* 25, 956–983.
- Rahmati-Ilkhchi, M., Faryad, S.W., Holub, F., Košler, J., Frank, W., 2009. Magmatic and metamorphic evolution of the Shotor Kuh metamorphic complex (Central Iran). *International Journal of Earth Sciences*. <http://dx.doi.org/10.1007/s00531-009-0499-0>.
- Rahmati-Ilkhchi, M., Jerabek, P., Faryad, S.W., Koyi, H.A., 2010. Mid-Cimmerian, Early Alpine and Late Cenozoic orogenic events in the Shotor Kuh Metamorphic complex, Great Kavir Block, NE Iran. *Tectonophysics* 494, 101–117.

- Ramezani, J., Tucker, R.D., 2003. The Saghand region, central Iran: U–Pb geochronology, petrogenesis and implications for Gondwana tectonics. *American Journal of Science* 303, 622–665.
- Reilinger, R., McClusky, S., Vernant, P., et al., 2006. GPS constraints on continental deformation in the Africa–Arabia–Eurasia continental collision zone and implications for the dynamics of plate interactions. *Journal of Geophysical Research* B05411. <http://dx.doi.org/10.1029/2005JB004051>.
- Robertson, A.H.F., Dixon, J.E., 1984. Introduction: aspects of the geological evolution of the Eastern Mediterranean. In: Dixon, J.E., Robertson, A.H.F. (Eds.), *The Geological Evolution of the Eastern Mediterranean*. Geological Society of London, Special Publication, no. 17, pp. 1–74.
- Rubatto, D., 2002. Zircon trace element geochemistry: partitioning with garnet and the link between U–Pb ages and metamorphism. *Chemical Geology* 184, 123–138.
- Rubatto, D., Hermann, J., Berger, A., Engi, M., 2009. Protracted fluid-induced melting during Barrovian metamorphism in the Central Alps. *Contributions to Mineralogy and Petrology* 155. <http://dx.doi.org/10.1007/s00410-009-0406-5>.
- Şengör, A.M.C., 1984. The Cimmeride orogenic system and the tectonics of Eurasia. *Geological Society of America Special Paper* (195 pp.).
- Şengör, A.M.C., 1987. Cross-faults and differential stretching of hanging walls in regions of low-angle normal faulting: examples from western Turkey. In: Coward, M.P., Dewey, J.F., Hancock, P.L. (Eds.), *Continental Extensional Tectonics*. Geological Society Special Publication, No. 28, pp. 575–589.
- Şengör, A.M.C., Natalin, B.A., 1996. Paleotectonics of Asia: fragment of a synthesis. In: Yin, A., Harrison, T.M. (Eds.), *The Tectonic Evolution of Asia*. Cambridge University Press, Cambridge, pp. 486–640.
- Shafaii Moghadam, H., Stern, R.J., 2011. Geodynamic evolution of upper Cretaceous Zagros ophiolites: formation of oceanic lithosphere above a nascent subduction zone. *Geological Magazine* 148, 762–801.
- Shafaii Moghadam, H., Ghorbani, G., Zaki Khedr, M., Fazlînia, N., Chiaradia, M., Eyuboglu, Y., Santosh, M., Galindo Francisco, C., Lopez Martinez, M., Gourgand, A., Arai, M., 2014. Late Miocene K-rich volcanism in the Eslamieh Peninsula (Saray), NW Iran: Implications for geodynamic evolution of the Turkish–Iranian High Plateau. *Gondwana Research* 26, 1028–1050.
- Shahabpour, J., 2007. Island-arc affinity of the central Iranian volcanic belt. *Journal of Asian Earth Sciences* 30, 652–665. <http://dx.doi.org/10.1016/j.jseas.2007.02.004>.
- Stampfli, G.M., 2000. Tethyan oceans. In: Bozkurt, E., Winchester, J.A., Piper, J.D. (Eds.), *Tectonics and Magmatism in Turkey and Surrounding Area*. Geological Society, London, Special Publications, 173, pp. 1–23.
- Stampfli, G.M., von Raumer, J., Borel, G., 2002. The Paleozoic evolution of pre Variscan terranes: from Gondwana to the Variscan collision. *Geological Society of America, Special Paper* 364, 263–280.
- Stern, R.J., 1994a. Arc assembly and continental collision in the Neoproterozoic East African Orogen: implications for the consolidation of Gondwanaland. *Annual Review of Earth and Planetary Sciences* 22, 319–351.
- Stern, R.J., 1994b. Neoproterozoic (900–550 Ma) Arc Assembly and continental collision in the East African Orogen. *Annual Review of Earth and Planetary Sciences* 22, 319–351.
- Stern, R.J., 2002. Crustal evolution in the East African Orogen: a neodymium isotopic perspective. *Journal of African Earth Sciences* 34, 109–117.
- Stern, R.J., 2008. Neoproterozoic crustal growth: the solid Earth system during a critical episode of Earth history. *Gondwana Research* 14, 33–50.
- Stern, R.J., Johnson, P., 2010. Continental lithosphere of the Arabian Plate: a geologic, petrologic, and geophysical synthesis. *Earth Science Reviews* 101, 29–67.
- Stöcklin, J., 1968. Structural history and tectonics of Iran: a review. *American Association of Petroleum Geologists Bulletin* 52, 1229–1258.
- Stöcklin, J., 1974. Possible ancient continental margin in Iran. In: Burk, C.A., Drake, C.L. (Eds.), *The Geology of Continental Margins*. Springer, Berlin, pp. 873–887.
- Strecheisen, A., 1974. Classification and nomenclature of plutonic rocks. *Geological Rundschau* 63, 773–786.
- Sun, S.S., McDonough, W.E., 1989. Chemical and isotopic systematics of oceanic basalts: implications for mantle composition and processes. In: Saunders, A.D., Norry, M.J. (Eds.), *Magmatism in the Ocean Basins*. Geological Society of London, Special Publication, pp. 313–345.
- Ustaömer, P.A., Mundil, R., Renne, P.R., 2005. U/Pb and Pb/Pb zircon ages for arc-related intrusions of the Bolu Massif (W Pontides, NW Turkey): evidence for Late Precambrian (Cadomian) age. *Terra Nova* 17, 215–223.
- Ustaömer, P.A., Ustaömer, T., Collins, A.S., Robertson, A.H.F., 2009. Cadomian (Ediacaran–Cambrian) arc magmatism in the Bitlis Massif, SE Turkey: magmatism along the developing northern margin of Gondwana. *Tectonophysics* 473, 99–112.
- Ustaömer, P.A., Ustaömer, T., Gerdes, A., Zulauf, G., 2011. Detrital zircon ages from a Lower Ordovician quartzite of the Istanbul exotic terrane (NW Turkey): evidence for Amazonian affinity. *International Journal of Earth Sciences* 100 (23), 41.
- Ustaömer, P.A., Ustaömer, T., Robertson, A.H.F., 2012. Ion probe U–Pb dating of the Central Sakarya basement: a peri-Gondwana terrane intruded by Late Lower Carboniferous subduction/collision-related granitic rocks. *Turkish Journal of Earth Sciences* 21, 905–932.
- Verdel, C., Wernicke, B.P., Ramezani, J., Hassanzadeh, J., Renne, P.R., Spell, T.L., 2007. Geology and thermochronology of Tertiary Cordilleran-style metamorphic core complexes in the Saghand region of central Iran. *Geological Society of America Bulletin* 119, 961–977. <http://dx.doi.org/10.1130/B26102.1>.
- Vervoort, J.D., Blichert-Toft, J., 1999. Evolution of the depleted mantle: Hf isotope evidence from juvenile rocks through time. *Geochimica et Cosmochimica Acta* 63, 533–556.
- Wang, Y., Zhang, F.F., Fan, W.M., Zhang, G.W., Chen, S.Y., Cawood, P.A., Zhang, A.M., 2010. Tectonic setting of the South China Block in the early Paleozoic: resolving intracontinental and ocean closure models from detrital zircon U–Pb geochronology. *Tectonics* 29, TC6020. <http://dx.doi.org/10.1029/2010TC002750>.
- Wu, Y.B., Zheng, Y.F., 2004. Genesis of zircon and its constraints on interpretation of U–Pb age. *Chinese Science Bulletin* 49, 1554–1569.
- Wu, Y.B., Zheng, Y.F., Zhang, S.B., Zhao, Z.F., Wu, F.Y., Liu, X.M., 2007. Zircon U–Pb ages and Hf isotope compositions of migmatite from the North Dabie terrane in China: constraints on partial melting. *Journal of Metamorphic Geology* 25, 991–1009.
- Yilmaz Sahin, S., Aysal, N., Güngör, Y., Peytcheva, I., Neubauer, F., 2014. Geochemistry and U–Pb zircon geochronology of metagranites in Istranca (Strandja) zone, NW Pontides, Turkey: Implications for the geodynamic evolution of Cadomian Orogeny. *Gondwana Research* 26, 755–771.
- Zhou, J.B., Zhou, S.A., Wilde, Zhang, X.Z., Zhao, G.C., Zheng, C.Q., Wang, Y.J., Zhang, X.H., 2009. The onset of Pacific margin accretion in NE China: evidence from the Heilongjiang high-pressure metamorphic belt. *Tectonophysics* 230–246.